Research Article

Jagadeesh Babu Kamili, Rabah W. Aldhaheri*, Anveshkumar Nella*, Khalid H. Alharbi, and Muntasir M. Sheikh

A novel gold and SiO_2 material based planar 5-element high HPBW end-fire antenna array for 300 GHz applications

https://doi.org/10.1515/phys-2024-0116
received October 01, 2024; accepted January 10, 2025

Abstract: This article is intended to propose a novel gold and SiO_2 material based planar 5-element high half power beam-width (HPBW) end-fire antenna array for 300 GHz applications. The proposed radiating structure composes of a 5-element off-set feed rectangular patch antenna array fed by a tapered microstrip line to accomplish high HPBW. Off-set feeding and parasitic patch resonators are incorporated to access the end-fire radiation characteristics. This antenna operating frequency ranges from 277.5 to 315 GHz with a peak gain and HPBW of the antenna as 4.98 dBi and around 100°, respectively, at 300 GHz, making it a good radiator at the specified band. A gold material of thickness 5 μm is used as the metal, while the SiO_2 with a thickness of 60 μm is adopted for the substrate material. Design, parametric analysis, and lumped element circuit models are also explored in this work. End-fire pattern, high HPBW, and good performance make this antenna to be eligible to use in THz applications such as imaging, scanning, communication, and bio-medical.

Keywords: end-fire antenna array, gold, HPBW, off-set feed, radiation pattern, SiO_2

*** Corresponding author: Rabah W. Aldhaheri,** Department of Electrical and Computer Engineering, King Abdulaziz University, Jeddah, 21589, Saudi Arabia, e-mail: raldhaheri@kau.edu.sa
*** Corresponding author: Anveshkumar Nella,** School of EEE, VIT Bhopal University, Kothri Kalan, Sehore, 466114, India, e-mail: nellaanvesh@gmail.com
Jagadeesh Babu Kamili: Department of ECE, St. Ann's College of Engineering and Technology, Chirala, India, e-mail: jagan_ec@yahoo.com
Khalid H. Alharbi: Department of Electrical and Computer Engineering, King Abdulaziz University, Jeddah, 21589, Saudi Arabia, e-mail: khalharbi@kau.edu.sa
Muntasir M. Sheikh: Department of Electrical and Computer Engineering, King Abdulaziz University, Jeddah, 21589, Saudi Arabia, e-mail: mshaikh@kau.edu.sa

1 Introduction

Nowadays, terahertz (THz) frequency radiation has grabbed significant attention for its high data rates in wireless communications. Therefore, many broadband communication systems are currently being developed in the THz frequency range [1–6]. But Lossy propagation and high-power shortage are the issues associated with the THz frequencies. Antennas radiating in end-fire direction find several applications in the present advanced wireless communications. The short pulses, ultra-high-frequency carriers, and the very high bandwidth of the THz spectrum are able to revolutionize the today's wireless communication by achieving maximum data rates of 100 GB/s [4]. As a result, the wireless data traffic, which is increasing exponentially, can be solved significantly [5]. Since THz frequencies have extremely small wavelengths and coherent non-ionizing property, the techniques used at THz are useful to facilitate high-resolution imaging and positioning, mainly for security and scanning the human body [6].

In the mentioned THz systems, the end-fire radiation antennas are the vital components to launch the electromagnetic energy into free space. A few finest end-fire antennas such as traveling wave antennas, Yagi-Uda antennas, substrate-integrated waveguide (SIW) antennas, and horn antennas, exist at THz bands as well. Horn antennas, which have advantages of simple structure, high gain, and wide band characteristics, have been reported in the literature at THz bands [7–11]. A 3D horn antenna that operates at 325–500 GHz was proposed in Fan *et al.* [9]. The radiation aperture of the horn antenna in E-plane and H-plane was enlarged for enhancing gain by employing a quasi-planar reflector. A dual polarized horn antenna was reported in Liang *et al.* [11]. To increase the impedance matching in its operational frequency band (*i.e.*, 220–330 GHz), effective medium lens was introduced. Reported horn antennas at THz frequencies require complex fabrication procedures such as deep reactive ion etching and computer numerical

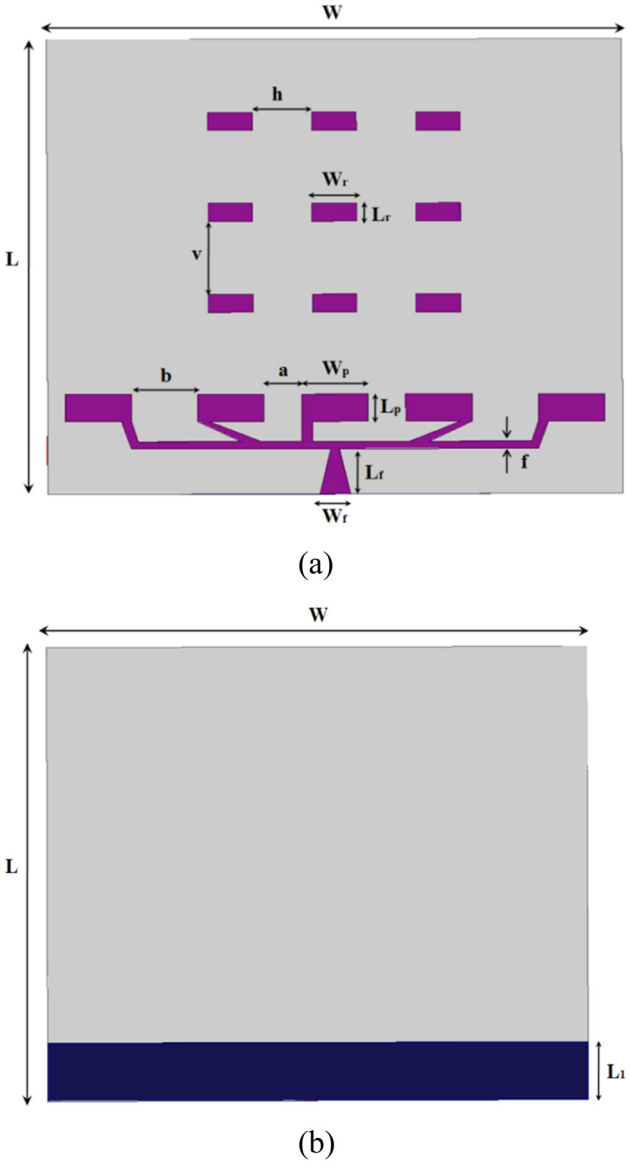

Figure 1: Proposed antenna: (a) top view and (b) bottom view.

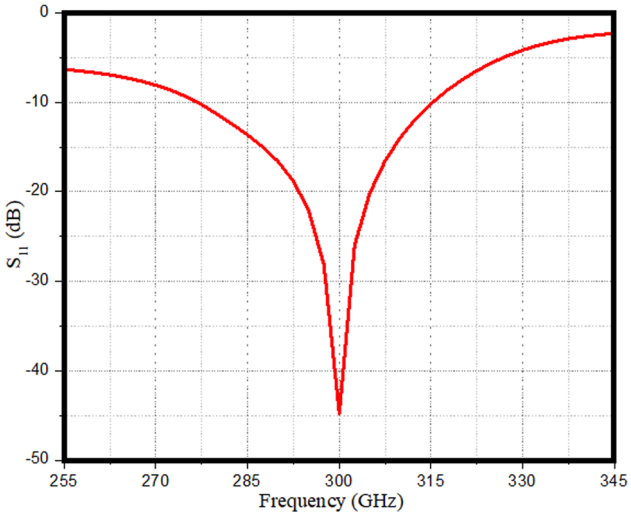

Figure 2: S_{11}-parameter of proposed antenna.

control matching. Moreover, integration with other planar terahertz components is difficult as waveguides are used for exciting them.

SIWs are also used for microwave applications similar to waveguides. This technology is applied to design antennas with end-fire radiation at microwave and millimeter wave frequencies [12–16]. An end-fire SIW antenna, which operates at 26.6–38.7 GHz, was proposed in Li and Chen [13]. It achieved wideband characteristics by loading two face rectangular-shaped patches, which act as a meta-surface. A SIW antenna with circular polarization characteristic at Ka band was reported in Wang *et al.* [15]. Two antipodal notches were etched to make a complementary source. Also, to increase the gain of the antenna in the end-fire direction, a dielectric rod-like structure was loaded. Even though the SIW antennas have some advantageous characteristics at microwave and millimeter wave frequencies, they are very difficult to fabricate at THz frequencies due to the presence of metallic vials. Hence, they are very limited at THz frequencies.

Another category of antennas known for generating end-fire radiation are Yagi-Uda antennas [17–20]. In the study by Deal *et al.* [17], a novel quasi-Yagi antenna is proposed using active planar array method. They comprise many directors, a reflector, and a driven element. This antenna achieves a measured 48% frequency bandwidth with 12 front-to-back-ratio (FBR), and less than-15 dB cross-polarization, and 3–5 dBi of absolute gain. In the study by Hu *et al.* [18], a vertically polarized top hat monopole Yagi-Uda antenna that operates at 0.55 GHz was presented. The folded top hat monopole acts as a driven element, whereas the four short-circuit monopoles act as directors. A Yagi-Uda antenna, which has an impedance bandwidth of 10 GHz, was

Table 1: Dimensions of the proposed antenna

Parameter	*W*	*L*	W_r	L_r	L_f	L_1	*v*	*h*	*a*	*b*	*f*
Size (mm)	1.3	1.25	0.1	0.05	0.125	0.16	0.2	0.135	0.085	0.15	0.002

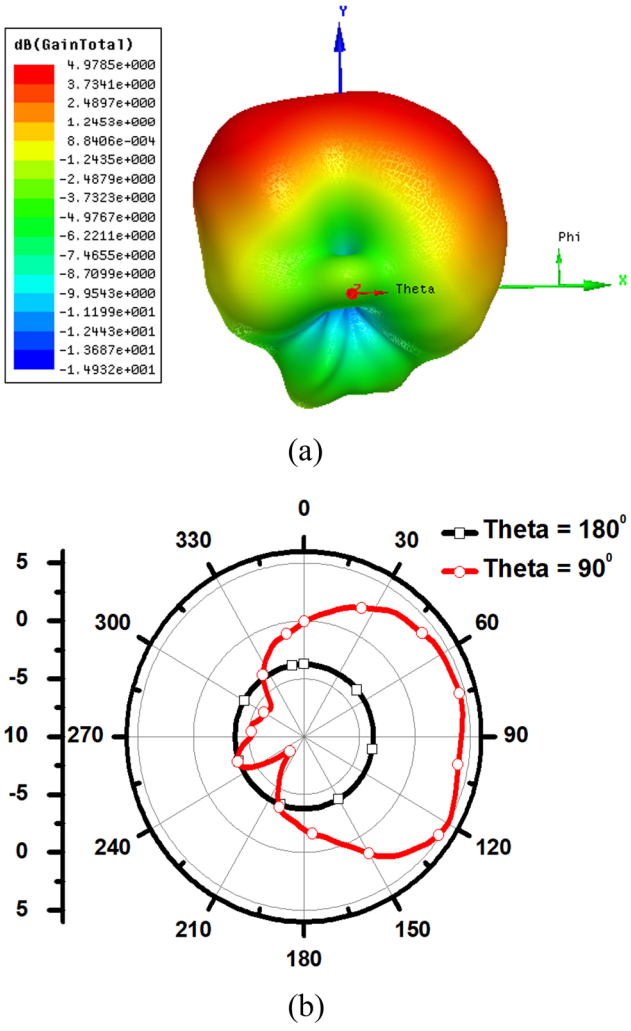

Figure 3: Radiation patterns at 300 GHz: (a) 3-D and (b) 2-D.

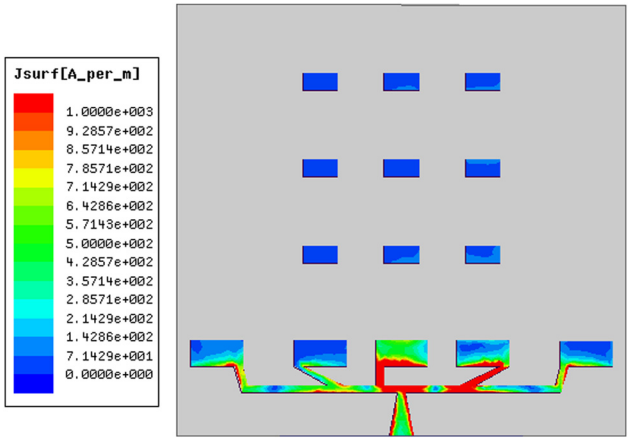

Figure 4: Surface current distribution at 300 GHz.

presented in Pavanello *et al.* [19]. A transition balun, which originates from a co-planar waveguide to a co-planar stripline at a frequency of 300 GHz, is used to excite the antenna. Moreover, the antenna was planar and was fabricated on a cyclic olefin co-polymer film, which has a thickness of 100 μ m. In the study by Wang *et al.* [20], a compact shared aperture antenna with high isolation characteristics is developed. The antenna is shown to give a peak radiation efficiency of 80%. This antenna uses the concept of combining monopole and dipole concept involving reconfigurable concept.

Another class of antennas that produces end-fire radiation is traveling wave antenna. It is generally based on a condition given by Hansen-Woodyard. The propagation constant of the antenna is typically needed to be more than the free space wavenumber slightly [21–25]. In the study by Hou *et al.* [22], a periodic leaky wave antenna with air as substrate is fed by a microstrip line. It has end-fire radiation characteristic and phase constant is manipulated by employing multiple monopoles. A traveling wave antenna was proposed in the study by Ge *et al.* [24] with end-fire radiation characteristic. It comprises crossover structures for phase reversal and satisfies the Hansen-Woodyard condition. As a result, it radiates electromagnetic energy into the free space constructively in the end-fire direction. The above-mentioned traveling wave antennas and Yagi-Uda antennas have some drawbacks such as limited bandwidth, complex 3-D geometries, and delicate structures with very thin substrates. Some other related works are also discussed in the available literature [26–32]. Moreover, none of the reported antenna structures in the literature has high HPBW. Hence, this article proposes a novel compact, lightweight, cost-effective, simple planar, and high performance 5-element off-set feed high HPBW end-fire antenna array for 300 GHz applications. This design adopts novelty by constructing a radiator with 5-element off-set feed rectangular patch antenna array fed by a tapered feedline to obtain high HPBW. This article is organized as follows: Section 2 reports the proposed antenna design, performance characteristics, equivalent model, and discussion. Section 3 presents the design steps, parametric variation, and results analysis. Section 4 concludes the work.

2 Proposed high HPBW antenna structure

In this design, gold of thickness 5 μm and silicon dioxide (SiO_2) of thickness 60 μm are used as metal and dielectric substrate, respectively. Top and bottom layers of the proposed antenna are shown in Figure 1(a) and (b), respectively. Overall dimensions ($L \times W$) of the antenna are 1.25 × 1.3 mm^2.

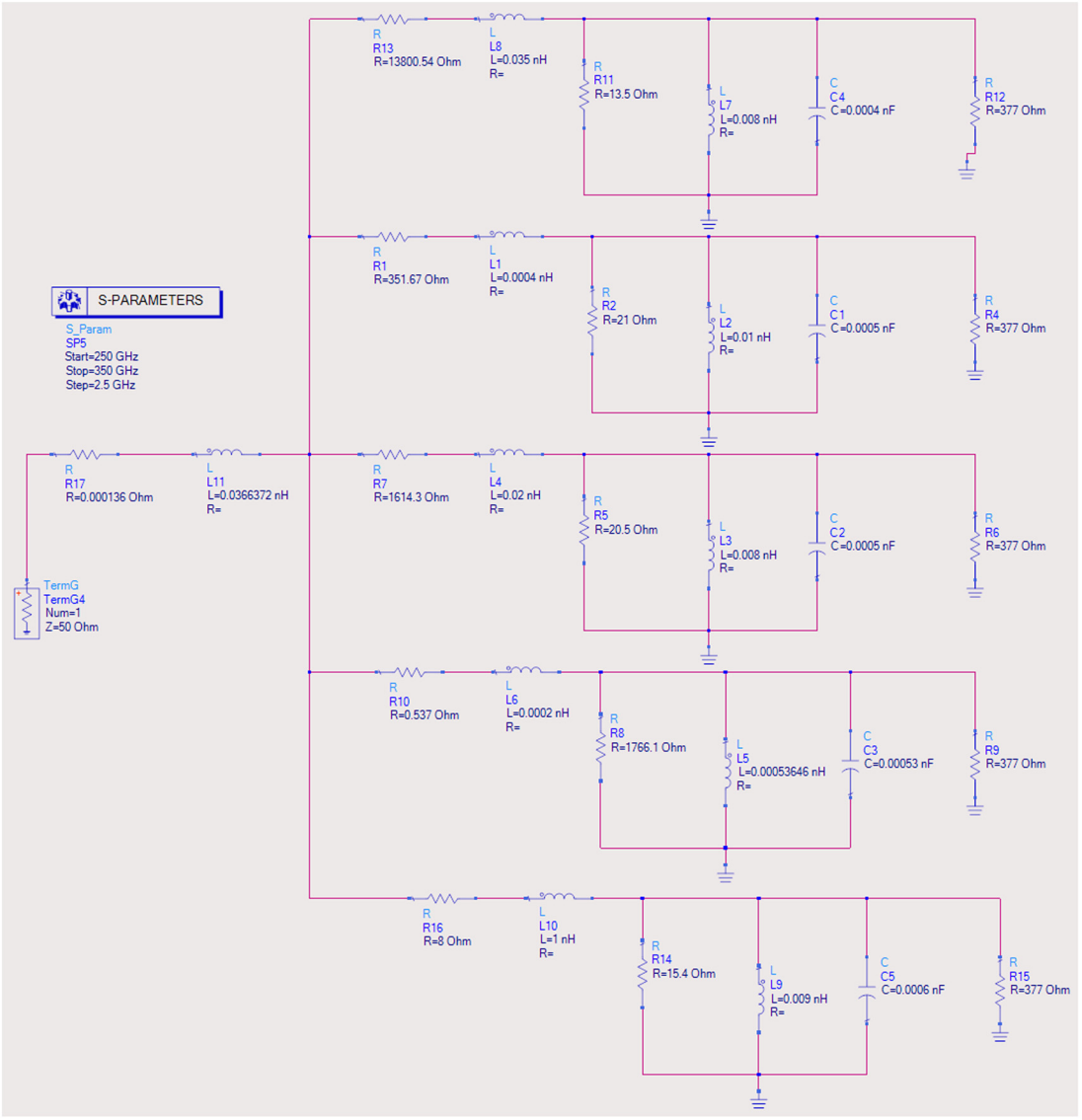

(a)

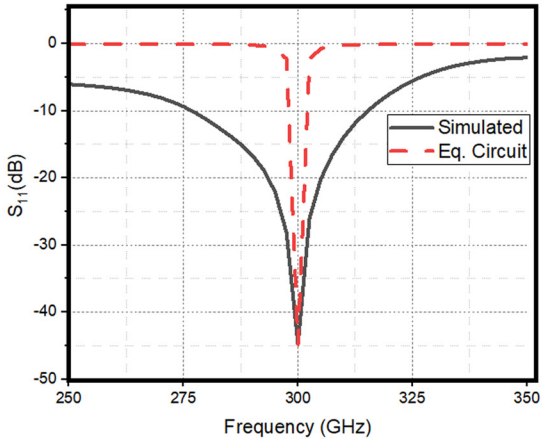

(b)

Figure 5: (a) Proposed antenna equivalent circuit model and (b) S-parameter performance.

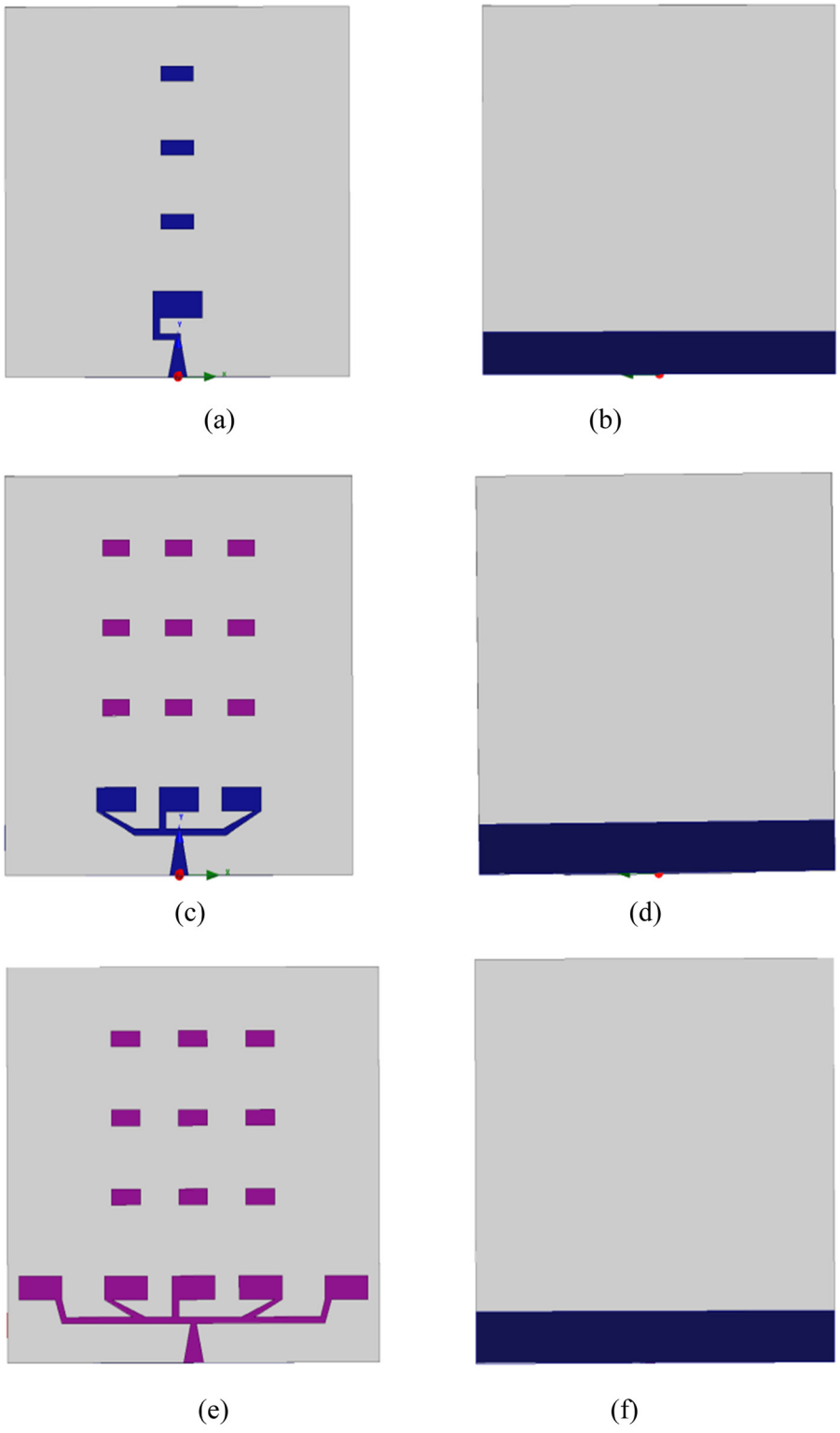

Figure 6: Evolution design steps (a) and (b) Design 1 (c) and (d) Design 2 (e) and (f) Design 3 (proposed antenna).

In the radiating structure, each patch element ($L_p \times W_p$) is of size 0.075 mm × 0.15 mm, while the feed line length (L_f) is 0.125 mm. Each parasitic resonator ($L_r \times W_r$) is with 0.05 mm × 0.1 mm, and partial ground has a length (L_1) of 0.16 mm. Spacing between the parasitic elements along horizontal direction (h) is 0.135 mm, while that along

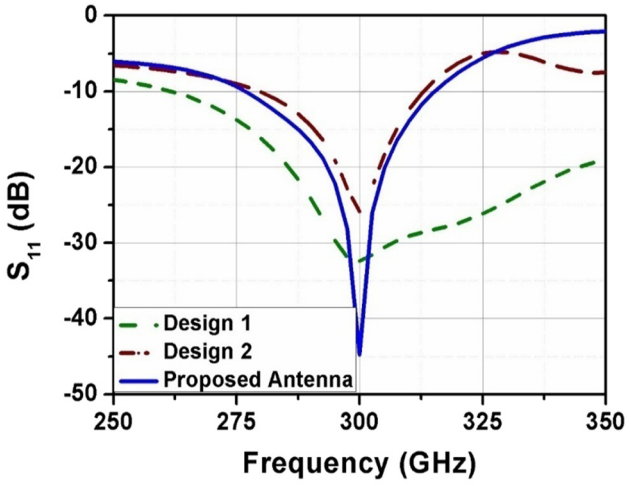

Figure 7: Reflection coefficient performance of the design steps.

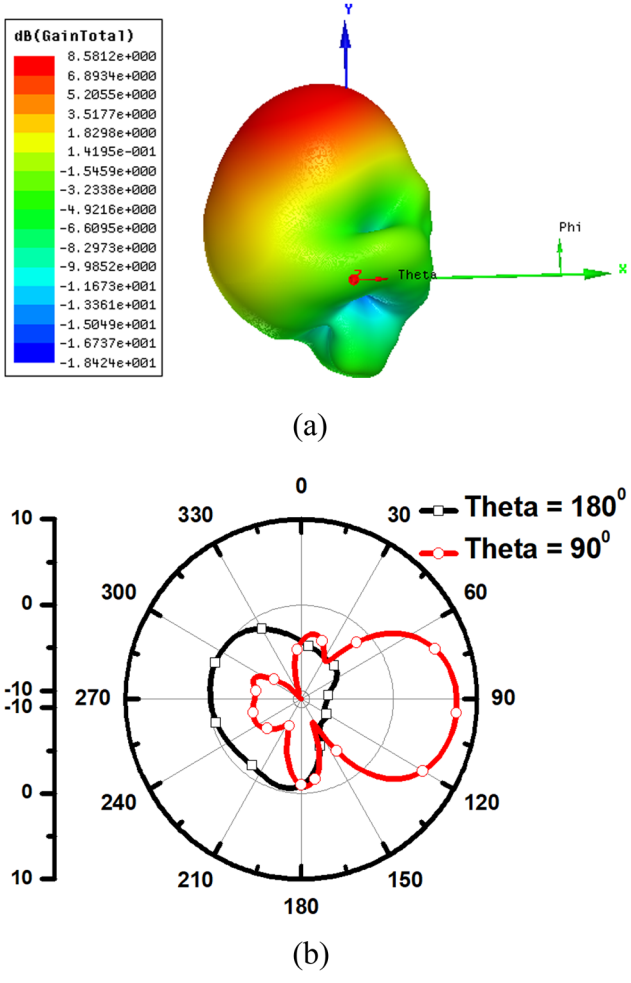

Figure 8: Radiation patterns at 300 GHz for Design 1: (a) 3-D and (b) 2-D.

vertical direction (v) is 0.2 mm. All the specified dimensions are mentioned in Table 1.

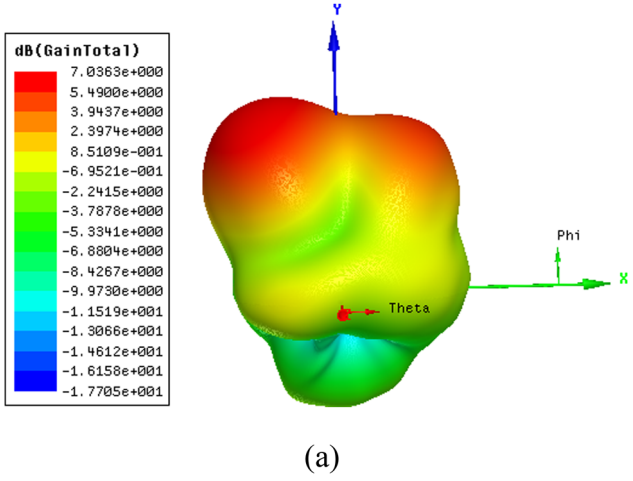

Figure 9: Radiation patterns at 300 GHz for Design 2: (a) 3-D and (b) 2-D.

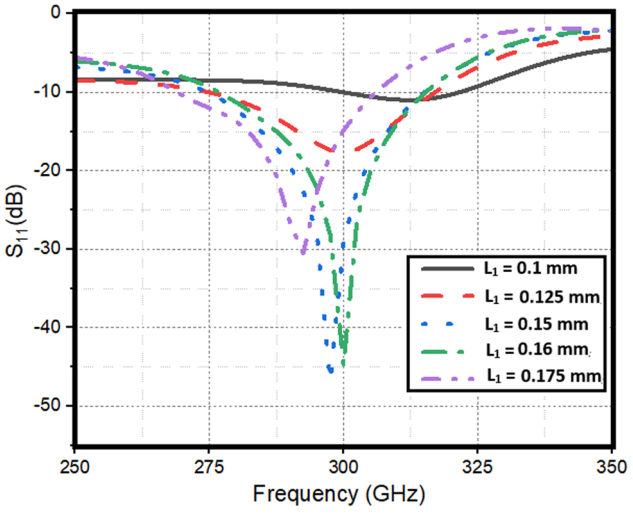

Figure 10: S_{11}-parameter variation w.r.t ground length (L_1).

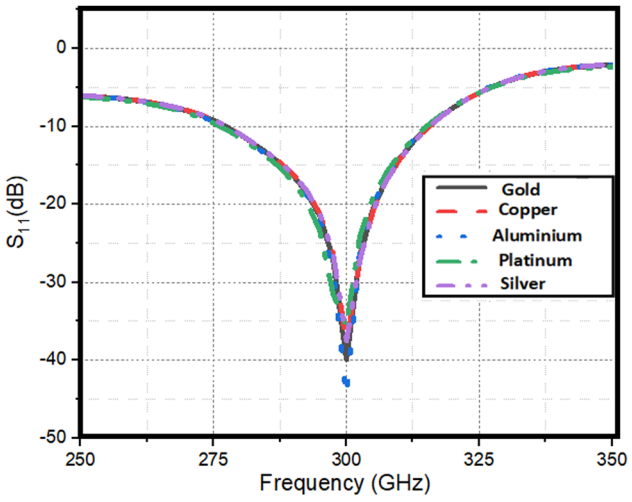

Figure 11: S_{11}-parameter variation w.r.t to metal.

The scattering parameters of this developed antenna are presented in Figure 2. Figure 2 depicts that the antenna is operating in a frequency range between 277.5 and 315 GHz with a resonant frequency at 300 GHz.

3D-radiation pattern is shown in Figure 3(a), while the 2D-pattern is shown in Figure 3(b). The 3D-pattern in Figure 3(a) presents a peak gain of 4.98 dBi at 300 GHz with end-fire radiation pattern. The 2D-pattern in Figure 3(b) reveals high HPBW of around 100°. Surface current distribution on the proposed antenna at 300 GHz is also shown in Figure 4. Hence, it is evident that the strong surface currents are almost residing uniformly in the patch antenna array elements.

A lumped element equivalent model of the proposed antenna is shown in Figure 5. This circuit model is developed on the basis of conventional approach to approximate a microstrip antenna using R, L, and C model. In general, the feed line is assumed as a series combination of R and L. The antenna radiator is denoted using a series combination of R, L while a parallel combination of R, L, and C is considered between the top and bottom planes. Hence, in the proposed 5-element antenna array, each element is represented using a series R, L and a parallel R, L, and C, as shown in Figure 5(a). Moreover, each antenna element is terminated with a free-space impedance of 377 Ω. The equivalent model design, optimization, and performance study are executed using ADS tool. The quality of the presented image can be enhanced using the image preprocessing techniques such as discussed in the study by Versaci *et al.* [33], where fuzzy logic is used for better image quality. However, for brevity, the lumped model of the image is presented here. In this model, each parameter is tuned over a range of values so that overall model S-parameter performance matches with the antenna performance as shown in Figure 5(b). From the figure, it is observed that S_{11}-parameter values of both simulated and equivalent circuit model take same resonance, however giving different impedance bandwidth values.

3 Design steps and parametric study

This section presents the design steps to realize the proposed antenna. This process follows three design steps. In the Design 1, an off-set fed monopole antenna with parasitic patch elements is designed with a tapered microstrip feed line as depicted in Figure 6(a) and (b). Off-set feeding mechanism is used to obtain the directional pattern in end-fire direction, while the parasitic patch elements are used to enhance the gain of the antenna. In the radiating structure, the patch element ($L_p \times W_p$) is of size 0.09 mm × 0.185 mm, while the feed line length (L_f) is 0.125 mm. Each parasitic resonator ($L_r \times W_r$) is with 0.05 mm × 0.123 mm, and partial ground has a length (L_1) of 0.145 mm. These dimensions are noted to obtain the resonant frequency at 300 GHz as shown in Figure 7. The Design 1 radiation 3D and 2D patterns are shown in Figure 8.

Table 2: Comparison with existing works

Ref.	Technique used	Resonant frequency (GHz)	Dimensions	HPBW
[26]	Dielectric cuboid	300	1 mm × 5.5 mm	17.6°
[27]	Horn antenna	300	3 mm × 3.5 mm	20°
[28]	Dielectric cuboid	300	1.36 mm × 1.36 mm	25°
[29]	SiGe patch	300	130 nm × 130 nm	—
[30]	Dielectric lens antenna	270	10 mm × 10 mm	7.4°
[31]	On chip horn	300	1 mm × 1.5 mm	20°
[32]	Vivaldi antenna	292	1.8 mm × 0.76 mm	—
This work	Microstrip patch	300	1.25 mm × 1.3 mm	100°

Peak gain of the antenna with this configuration is 8.58 dBi, as illustrated in Figure 8(a). Figure 8(b) also reveals that the pattern has less HPBW noting a narrow directional pattern. But the main objective of this design is to enhance the HPBW.

Hence, Design 2 is enhanced by adding three rectangular radiators using a tapered microstrip line, as depicted in Figure 6(c) and (d). In the radiating structure, the patch element ($L_p \times W_p$) is of size 0.075 mm × 0.148 mm, while each parasitic resonator ($L_r \times W_r$) is with 0.05 mm × 0.097 mm. A total of nine parasitic patch elements are used to get end-fire radiation characteristics. The -10 dB reflection coefficient bandwidth achieved with this configuration ranges from 280 to 313 GHz, as shown in Figure 7. The Design 2 radiation 3D and 2D patterns are shown in Figure 9. Peak gain of the antenna designed with this configuration is 7.03 dBi, as illustrated in Figure 9(a). It can be observed that the HPBW is enhanced, as depicted in Figure 9(b), due to the deployment of three patch elements. To further increase the HPBW, five rectangular radiators are fed by a tapered microstrip line, as depicted in Figure 1(a).

An important observation in this present work is the study of S_{11}-parameters on ground length variation and material changes. The impact of ground length L_1 on the variation of S_{11}-parameters is studied and portrayed in Figure 10. From the figure, it is obvious that for L_1 = 0.16 mm, better reflection coefficient values are obtained compared to the other values of L_1 such as 0.1, 0.125, 0.15, and 0.175 mm. Hence, in the design of this antenna, the value of L_1 considered is 0.16 mm, giving better return loss. Another important parameter to study in the present work is to know the impact of material selected on the reflection coefficient values of the designed antenna as the chosen material may affect the antenna's radiation properties at THz frequencies. The variation of S_{11}-parameters on the material used in the antenna is presented in Figure 11. From the figure, it is clearly seen that at the chosen THz frequencies, the material has almost no impact on the reflection coefficient values, and hence, in this study, gold is selected in the design of the antenna.

The proposed work is compared with some existing antennas in the literature as in Table 2. In the study by Ohno *et al.* [26], a novel phased array of dielectric cuboid is designed at 300 GHz having a size of 1 mm × 5.5 mm. In the study by Rey *et al.* [27], a phased array of horn antenna operating at 300 GHz is designed. The antenna has an overall size of 3 mm × 3.5 mm with HPBW of 20°. In the study by Yamada *et al.* [28], another cuboid antenna operating at 300 GHz is designed with a size of 1.36 mm × 1.36 mm and HPBW of 25°. In the study by Zheng *et al.* [29], a 130 nm × 130 nm sized SiGe patch antenna operating at 300 GHz is designed and developed. In the study by Ishihara *et al.* [30], lens-based dielectric antenna with 10 mm × 10 mm dimension is designed. The proposed antenna covers the band 277.5–315 GHz with dimensions 1.25 mm × 1.3 mm, and HPBW of 100° is designed and developed.

4 Conclusion

A novel planar HPBW 5-element end-fire antenna array for 300 GHz applications has been presented. It has a fractional bandwidth of 12.6% and a peak gain of 4.98 dBi. Design steps, parametric variation, and equivalent circuit model have also been presented. It is very advantageous at 300 GHz applications where high HPBW and end-fire radiation patterns are major concerns. Moreover, the antenna design is simple, planar and obtains good directional performance. Hence, the structure can find its THz applications, including THz imaging, scanning, communication, and security.

Funding information: This work was funded by the Deanship of Scientific Research (DSR) at King Abdulaziz University, Jeddah, Saudi Arabia, under Grant No (RG-46-135-42).

Author contributions: The conceptualization, simulation, and experimental part were carried out by A. K. N. Conceptualization, methodology, and supervising the research were done by R. W. A. The manuscript preparation and part of simulations were carried out by J. B. K. Result validation and formal analysis were carried out by K.H.A. and M.M.S. All authors have read and agreed to the published version of this manuscript, design of the study; in the collection, analyses, or interpretation of data; in the writing of the manuscript, or in the decision to publish the results. All authors have accepted responsibility for the entire content of this manuscript and approved its submission.

Conflict of interest: The authors state no conflict of interest.

Data availability statement: All data generated or analyzed during this study are included in this published article.

References

[1] Siegel PH. Terahertz technology in biology and medicine. IEEE Trans Microw Theory Tech. Oct 2004;52(10):2438–47.

[2] Balanis CA. Antenna theory: Analysis and design. Hoboken, NJ, USA: Wiley; 2016.
[3] Song H-J, Nagatsuma T. Present and future of terahertz communications. IEEE Trans Terahertz Sci Technol. Sep 2011;1(1):256–63, 481.
[4] Elayan H, Amin O, Shihada B, Shubair RM, Alouini M-S. Terahertz band: The last piece of RF spectrum puzzle for communication systems. IEEE Open J Commun Soc. 2020;1:1–32.
[5] Rodriguez-Vazquez P, Grzyb J, Heinemann B, Pfeiffer UR. A QPSK 110-Gb/s polarization-diversity MIMO wireless link with a 220–255 GHz tunable LO in a SiGe HBT technology. IEEE Trans Microw Theory Tech. Sep 2020;68(9):3834–51.
[6] Sarieddeen H, Saeed N, Al-Naffouri TY, Alouini M-S. Next generation terahertz communications: A rendezvous of sensing, imaging, and localization. IEEE Commun Mag. May 2020;58(5):69–75.
[7] Liu Y, Lu H, Wu Y, Cui M, Li B, Zhao P, et al. Millimeter wave and terahertz waveguide-fed circularly polarized antipodal curvedly tapered slot antennas. IEEE Trans Antennas Propag. May 2016;64(5):1607–14.
[8] Sekiguchi S, Sugimoto M, Shu S, Sekimoto Y, Mitsui K, Nishino T, et al. Broadband corrugated horn array with direct machined fabrication. IEEE Trans Terahertz Sci Technol. Jan 2017;7(1):36–41.
[9] Fan K, Hao Z-C, Yuan Q, Hong W. Development of a high gain 325–500 GHz antenna using quasi-planar reflectors. IEEE Trans Antennas Propag. Jul 2017;65(7):3384–91.
[10] Gonzalez A, Kaneko K, Asayama S. 1.25–1.57 THz dual polarization receiver optics based on corrugated horns. IEEE Trans Terahertz Sci Technol. May 2018;8(3):321–8.
[11] Liang J, Gao W, Lees H, Withayachumnankul W. All-silicon terahertz planar horn antenna. IEEE Antennas Wirel Propag Lett. 508 Nov 2021;20(11):2181–5.
[12] Taringou F, Dousset D, Bornemann J, Wu K. Broadband CPW feed for millimeter-wave SIW-based antipodal linearly tapered slot antennas. IEEE Trans Antennas Propag. Apr 2013;61(4):1756–62.
[13] Li T, Chen ZN. Wideband substrate-integrated waveguide-fed endfire metasurface antenna array. IEEE Trans Antennas Propag. Dec 2018;66(12):7032–40.
[14] Wu Q, Hirokawa J, Yin J, Yu C, Wang H, Hong W. Millimeter wave multibeam endfire dual-circularly polarized antenna array for 5G wireless applications. IEEE Trans Antennas Propag. Sep 2018;66(9):4930–5.
[15] Wang J, Li Y, Ge L, Wang J, Chen M, Zhang Z, et al. Millimeter-wave wideband circularly polarized planar complementary source antenna with endfire radiation. IEEE Trans Antennas Propag. Jul 2018;66(7):3317–26.
[16] Ruan X, Chan CH. An end fire circularly polarized complementary antenna array for 5G applications. IEEE Trans Antennas Propag. Jan 2020;68(1):266–74.
[17] Deal WR, Kaneda N, Sor J, Qian Y, Itoh T. A new quasi-Yagi antenna for planar active antenna arrays. IEEE Trans Microw Theory Tech. Jun 2000;48(6):910–8.
[18] Hu Z, Shen Z, Wu W, Lu J. Low-profile top-hat monopole Yagi antenna for end-fire radiation. IEEE Trans Antennas Propag. Dec 2015;63(12):5484–91.
[19] Pavanello F, Ducournau G, Peytavit E, Lepilliet S, Lampin J-F. High-gain Yagi–Uda antenna on cyclic olefin copolymer substrate for 300-GHz applications. IEEE Antennas Wirel Propag Lett. 2014;13:939–42.
[20] Wang Z, Ning Y, Dong Y. Compact shared aperture quasi-Yagi antenna with pattern diversity for 5G-NR applications. IEEE Trans Antennas Propag. Jul 2021;69(7):4178–83.
[21] Hou Y, Li Y, Zhang Z, Feng Z. Narrow-width periodic leaky-wave antenna array for endfire radiation based on Hansen–Woodyard condition. IEEE Trans Antennas Propag. Nov 2018;66(11):6393–6.
[22] Hou Y, Li Y, Zhang Z, Feng Z. High-gain leaky-wave end-fire antenna based on Hansen–Woodyard condition. IEEE Antennas Wirel Propag Lett. Oct 2019;18(10):2155–9.
[23] Ge S, Zhang Q, Rashid AK, Wang H, Murch RD. Design of high-gain and small-aperture endfire antenna using a phase-reversal technique. IEEE Trans Antennas Propag. Jul 2020;68(7):5142–50.
[24] Ge S, Zhang Q, Rashid AK, Zhang Y, Wang H, Murch RD. General design technique for high-gain traveling-wave endfire antennas using periodic arbitrary-phase loading technique. IEEE Trans Antennas Propag. Jun 2021;69(6):3094–105.
[25] Zhang X, Sun L, Li Y, Zhang Z. A grooved half-mode waveguide leaky-wave antenna for vertically-polarized endfire radiation. IEEE Trans Antennas Propag. Dec 2021;69(12):8229–36.
[26] Ohno T, Sakai R, Hisatake S. Phased array of dielectric cuboid antenna at 300 GHz band. International Symposium on Antennas and Propagation (ISAP), Sydney. Australia. 2022. p. 363–4.
[27] Rey S, Merkle T, Tessmann A, Kürner T. A phased array antenna with horn elements for 300 GHz communications. International Symposium on Antennas and Propagation (ISAP), Okinawa, Japan. 2016. p. 122–3.
[28] Yamada K, Samura Y, Minin OV, Kanno A, Sekine N, Nakajima J, et al. Short-range wireless transmitter using mesoscopic dielectric cuboid antenna in 300-GHz band. 50th European Microwave Conference (EuMC), Utrecht, Netherlands. 2021. p. 195–8.
[29] Zheng S, Tang S, Xia X, Zhou P, Chen J, Hong W. A 300 GHz SiGe patch antenna with 5.3 dBi gain using off-chip package. International Symposium on Antennas and Propagation (ISAP), Sydney, Australia. 2022. p. 209–10.
[30] Ishihara R, Sakakibara K, Kikuma N, Sugimoto Y, Yamada Y, Abd Rahman NH. Measured performance of high gain dielectric lens antenna in 300 GHz band. International Symposium on Antennas and Propagation (ISAP), Osaka, Japan. 2021. p. 17–8.
[31] Chen W-H, Ma T-G, Tsai J-H, Cheng Y-H. 300 GHz on-chip horn antenna with WR-03 to SIW transition using integrated passive device. IEEE International Symposium on Antennas and Propagation and USNC-URSI Radio Science Meeting (USNC-URSI), Portland, OR, USA. 2023. p. 429–30.
[32] Chen Z-F, Tu Z-H, Lin C-H, Cheng Y-H. 300 GHz low-cost PCB vivaldi antenna array and transition structure to WR-3 waveguide. IEEE Access. 2024;12:92169–74.
[33] Versaci M, Angiulli G, La Foresta F, Laganà F, Palumbo A. Intuitionistic fuzzy divergence for evaluating the mechanical stress state of steel plates subject to bi-axial loads. Integr Comput-Aided Eng. 2024;31(4):363–79.